EKF-based Predictive Stabilization of Shipboard DC Microgrids with Uncertain Time-varying Load

Yousefizadeh, Shirin; Bendtsen, Jan Dimon; Vafamand, Navid; Khooban, Mohammad Hassan; Dragicevic, Tomislav; Blåbjerg, Frede

Published in:
I E E E Journal of Emerging and Selected Topics in Power Electronics

DOI (link to publication from Publisher):
10.1109/JESTPE.2018.2889971

Publication date:
2019

Document Version
Accepted author manuscript, peer reviewed version

EKF-based Predictive Stabilization of Shipboard DC Microgrids with Uncertain Time-varying Load

Shirin Yousefizadeh, Jan Dimon Bendtsen, *Member, IEEE*, Navid Vafamand, Mohammad Hassan Khooban, *Senior Member, IEEE*, Tomislav Dragičević, *Senior Member, IEEE*, and Frede Blaabjerg, *Fellow, IEEE*

***Abstract*— The performance of DC shipboard power systems (SPSs) may degrade due to the negative impedance of constant power loads (CPLs) connected to DC microgrids (MGs). To control the DC SPS effectively, estimation of the instantaneous power flow to the time-varying uncertain CPLs is necessary. Furthermore, fast adaptive control is needed to deal with changes in the CPL power flow and quick stabilization of the DC MGs. Such a controller typically uses injection current from an energy storage system (ESS) for actuation. Since measuring the CPLs' powers require installing current sensors that are both costly and not optimal, an estimation of the CPLs' powers should be employed. In this paper, an extended Kalman filter (EKF) is developed to estimate a time-varying power of uncertain CPLs in a DC MG based on measuring capacitor voltages. The estimated power is then used in a Takagi-Sugeno (TS) fuzzy-based model predictive controller (MPC) to manipulate the energy storage unit. The proposed approach is tested experimentally on a DC MG that feeds a single CPL. The experimental results show that the proposed MPC controller alongside the developed EKF improves the transient performance and the stability margin of the DC MGs used in the SPSs.**

***Index Terms*— Shipboard power system, DC microgrid, Constant power load, Takagi-Sugeno fuzzy model, Model predictive control, Extended Kalman filter.**

I. INTRODUCTION

IN recent years, DC microgrids (MG) tend to be increasingly preferred over AC MGs in all-electric ships (AES) applications, due to various advantages including simple control, high efficiency and robustness, enhanced fault reconfigurability, and a simple common interface between distributed generations (DG) and electronic loads [1]–[3]. In recent years, several research projects have been focused on the deployment of medium-voltage DC MGs in ships, including the "Technological Development Roadmap" in USA [4] and the "MVDC Large Ships" in Europe [5], as well as the usage of low-voltage DC MGs in projects such as "EDisON-Efficient Distributed Onboard DC grid" [6]. A DC shipboard power system (SPS), which belongs to the class of islanded DC MGs, has several challenging stability and performance issues. These challenges mainly arise due to the existence of constant power loads (CPLs), which are produced by tight regulations of power electric converters connected to the loads [7]. The incremental negative impedance of the CPLs may degrade the DC MG stability or even cause system instability [7], [8]. Thus, in order to operate the DC MG effectively, it is required to minimize the destabilizing effect of CPLs. Several nonlinear control approaches have been reported in the literature regarding the stability problems of DC MGs containing CPLs [9] and alleviating the destabilizing effects of the CPLs in such systems [10]–[13]. In [9], a Takagi-Sugeno (TS) fuzzy model-based stability analysis is investigated. In [14], first, the Lipchitz technique is deployed to obtain a quasi-linear system from the nonlinear CPL dynamics to implement a robust linear controller. However, it is commonly assumed in the aforementioned studies that all CPLs are ideal. However, in practical applications, MGs contain uncertain and/or time-varying CPLs, which can not be regarded as ideal CPLs. A few papers have studied the effect of non-ideal CPLs effect on the stability of DC MGs [15]–[17]. In [15], after constructing a linear fractional transformation of an uncertain MG, μ-synthesis is used to calculate the maximum upper bound of the system uncertainties to guarantee system stability. In [16], sufficient stability conditions are derived in terms of LMIs under the assumption that the unknown power consumption of the CPLs are bounded by some pre-given limits. The authors of [17] proposed a sliding mode controller to stabilize a MG containing uncertain CPLs by means of an energy storage unit. Even though the proposed designs in [15]–[17] incorporate both stability and robustness, they all assume that the uncertainty in power consumption is bounded by a known constant. In practice, this bound is rarely known. In order to overcome the considered limit on CPLs power uncertainty, the prompt values of CPLs powers are needed. One option to this aim is integrating current and voltage sensors in the DC MG. However, series installation of currents sensors increases the output impedance and degrades ripple filtering

S. Yousefizadeh and J. D. Bendtsen are with the Department of Electronic Systems, Aalborg University, Aalborg 9220, Denmark (E-mails:,{shy, dimon}@es.aau.dk).

N. Vafamand is with Department of Power and Control Engineering, School of Electrical and Computer Engineering, Shiraz University, Shiraz 71348-51154, Iran and Department of Energy Technology, Aalborg University, Aalborg 9220, Denmark (E-mail: n.vafamand@shirazu.ac.ir.

M. H. Khooban, T. Dragičević and F. Blaabjerg are with Department of Energy Technology, Aalborg University, Aalborg 9220, Denmark (E-mails: {kho, tdr, fbl}@et.aau.dk).

This article has been accepted for publication in a future issue of this journal, but has not been fully edited. Content may change prior to final publication. Citation information: DOI 10.1109/JESTPE.2018.2889971, IEEE Journal of Emerging and Selected Topics in Power Electronics

[11]. Additionally, installing extra sensors increases system cost and complexity. Therefore, instead of employing sensors to obtain the CPLs' powers, estimation methods should be used. The two main approaches for unknown parameter estimation are deterministic observers and stochastic estimators. Deterministic observers treat the unknown parameters as disturbances. The equivalent disturbance is then estimated by minimizing the difference between the estimated output and the output of the nominal response model [18]. However, measurement noise may impair the deterministic observers' performance [19]. Extended Kalman filters, on the other hand, are known to be robust against noise effects [20]. A high performance control over system dynamic and operating point variations can be accomplished by employing an adaptive controller [21]. Therefore, to compensate for the CPLs' destabilizing effects, an online adaptive controller is required to modify the injecting current of the energy storage system (ESS) to match the estimated power of the CPLs. MPC is an effective and popular control approach that predicts the future behavior of a system over a specific prediction horizon and optimizes the input on a sample-by-sample basis [22], [23]. The online calculations can be carried out by e.g. quadratic optimization or by LMI-based techniques [24]. Adaptive model predictive control (AMPC) is based on updating the system model in real-time, which considers the control objectives to obtain the control signal as an optimal multi-objective control problem [25]. Nonlinear MPC problems can be formulated in terms of LMIs by considering TS fuzzy models [22]–[24]. A TS fuzzy model represents a complex nonlinear system by a set of fuzzy rules, where the consequent parts are linear state space equations. Then, the complex nonlinear system can be described as a nonlinearly weighted sum of these linear state equations [26].

In this paper, a novel adaptive MPC controller is employed to stabilize a DC SPS, which contains a DC MG connected to uncertain time-varying CPLs. To eliminate the destabilizing effects of CPLs in the SPS, the proposed approach first utilizes an EKF algorithm to estimate the instantaneous power of the CPLs, which is more economical and optimal than using sensors to measure the CPLs' powers. To do this, the CPLs' power consumptions are considered as virtual states and augmented in the system's state vector. The estimated CPLs' power consumptions are then feedforwarded into a TS fuzzy model-based MPC scheme to optimally stabilize the SPS DC MG through modifying the ESS injection current. Utilizing a TS fuzzy representation of the system enables employing a linear MPC controller, which yields guaranteed control performance and decreases the online computational burden. The developed adaptive controller is applied to a DC MG, which is connected to an uncertain time-varying CPL. The effectiveness of the proposed EKF to estimate the unknown time-varying CPL power and the Merged MPC controller with the EKF to stabilize the SPS DC MG are verified by real-time experiments.

The outline of this paper is as follows. The modeling of the DC MG is provided in Section II. In Section III, the developed EKF algorithm for unknown power estimation is presented. The TS fuzzy model-based MPC controller is presented in Section IV. To investigate the performance of the proposed estimator and controller, the illustrative experimental results are presented in sections V. Finally, Section VI concludes the paper.

II. SYSTEM CONFIGURATION AND MODELLING

A typical shipboard power system comprising several CPLs is shown in Fig. 1, and the corresponding circuit diagram is shown in Fig. 2. An example of CPLs in SPS is heaters, which are used to maintain the comfort in cold weather and to heat food. These heaters are required to keep the dissipated power form the heater constant in spite of process variations. Another example of CPLs is compressors, which are used to start engines, to operate ships whistle and valves, and so forth.

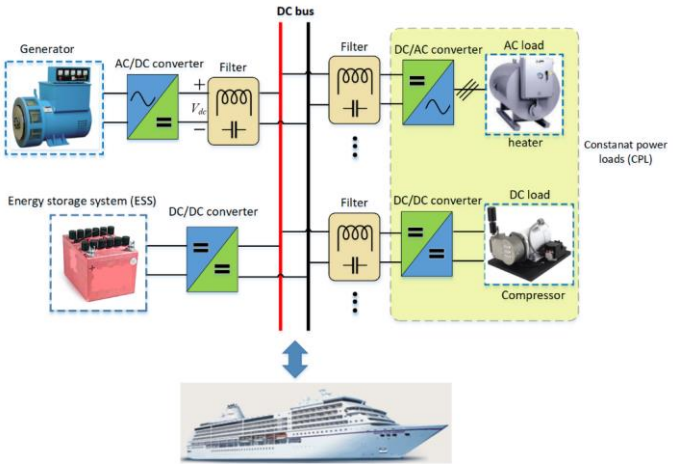

Fig. 1. Illustration of a shipboard power system DC MG.

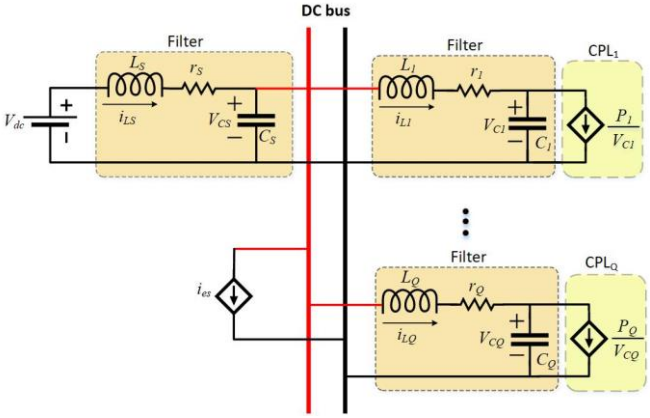

Fig. 2. An illustration of the SPS DC MG with Q CPLs.

The system shown in Fig. 2 consists of Q CPLs and one energy storage system (ESS). By employing Kirchhoff's current and voltage laws, the dynamic model of the j^{th} CPL is obtained as

$$\begin{cases} \dot{i}_{Lj} = -\dfrac{r_j}{L_j} i_{Lj} - \dfrac{1}{L_j} v_{Cj} + \dfrac{1}{L_j} V_{dc} \\ \dot{v}_{Cj} = \dfrac{1}{C_j} i_{Lj} - \dfrac{P_j}{C_j} \dfrac{1}{v_{cj}} \end{cases} , j = 1,2,\dots,Q \qquad (1)$$

where r_j, L_j, C_j are the output filter resistance, inductance and capacitance, respectively. V_{dc} is the DC voltage of the source,

This article has been accepted for publication in a future issue of this journal, but has not been fully edited. Content may change prior to final publication. Citation information: DOI 10.1109/JESTPE.2018.2889971, IEEE Journal of Emerging and Selected Topics in Power Electronics

P_j is the load power, and i_{Lj}, v_{Cj} are the inductor current and capacitor voltage of the output filter, respectively. Then, the dynamic model of all CPLs $(1, \dots, Q)$ can be obtained as

$$\begin{cases} \dot{x}_j = A_j x_j + d_j \rho_j + A_{js} x_s \\ y_j = h_j x_j \end{cases} \tag{2}$$

where $x_j = \begin{bmatrix} i_{Lj} & v_{Cj} \end{bmatrix}^T$ is the j^{th} CPL's state vector and

$$A_j = \begin{bmatrix} -\frac{r_j}{L_j} & -\frac{1}{L_j} \\ \frac{1}{C_j} & 0 \end{bmatrix}, d_j = \begin{bmatrix} 0 \\ \frac{-P_j}{C_j} \end{bmatrix}, A_{js} = \begin{bmatrix} 0 & \frac{1}{L_j} \\ 0 & 0 \end{bmatrix}, \quad h_j = [0 \quad 1], \rho_j = \frac{1}{v_{cj}} \tag{3}$$

Similarly, the dynamic model of the ESS is obtained as

$$\begin{cases} \dot{i}_{Ls} = -\frac{r_s}{L_s} i_{Ls} - \frac{1}{L_s} v_{Cs} + \frac{1}{L_s} V_{dc} \\ \dot{v}_{Cs} = \frac{1}{C_s} i_{Ls} - \frac{1}{C_s} i_{Lj} - \frac{1}{C_s} i_{es} \end{cases} \tag{4}$$

where r_s, L_s, C_s are the output filter resistance, inductance, and capacitance, respectively. i_{es} is the ESS injection current, and i_{Ls}, v_{Cs} are the inductor current and capacitor voltage of the input filter, respectively. This model can be rewritten as

$$\begin{cases} \dot{x}_s = A_s x_s + b_s V_{dc} + b_{es} i_{es} + \Sigma_{j=1}^{Q} A_{cn} x_j \\ y_s = h_s x_s \end{cases} \tag{5}$$

where $x_s = [i_{Ls} \quad v_{Cs}]^T$ is the ESS state vector, and

$$A_s = \begin{bmatrix} -\frac{r_s}{L_s} & -\frac{1}{L_s} \\ \frac{1}{C_s} & 0 \end{bmatrix}, b_s = \begin{bmatrix} \frac{1}{L_s} \\ 0 \end{bmatrix}, h_s = [0 \quad 1], \quad A_{cn} = \begin{bmatrix} 0 & 0 \\ \frac{-1}{C_s} & 0 \end{bmatrix}, b_{es} = \begin{bmatrix} 0 \\ -\frac{1}{C_s} \end{bmatrix} \tag{6}$$

By combining the CPL and source state vectors, the overall dynamic model of the DC MG is obtained as [14]:

$$\begin{cases} \dot{X} = \overline{A} X + D\rho + B_{es} i_{es} + B_s V_{dc} \\ Y = HX \end{cases} \tag{7}$$

where $X = \begin{bmatrix} x_1^T & x_2^T & \dots & x_Q^T & x_s^T \end{bmatrix}^T$, $\rho = \begin{bmatrix} \rho_1, \dots, \rho_Q \end{bmatrix}^T$, and

$$\overline{A} = \begin{bmatrix} A_1 & 0 & \dots & 0 & A_{1s} \\ 0 & A_2 & \cdots & 0 & A_{2s} \\ \vdots & \vdots & \ddots & \vdots & \vdots \\ 0 & 0 & \cdots & A_Q & A_{Qs} \\ A_{cn} & A_{cn} & \cdots & A_{cn} & A_s \end{bmatrix}, B_{es} = \begin{bmatrix} 0 \\ \vdots \\ 0 \\ b_{es} \end{bmatrix}, \quad B_s = \begin{bmatrix} 0 \\ \vdots \\ 0 \\ b_s \end{bmatrix}, D = \begin{bmatrix} d_1 & 0 & \dots & 0 \\ 0 & d_2 & \cdots & 0 \\ \vdots & \vdots & \ddots & \vdots \\ 0 & 0 & \cdots & d_Q \\ 0 & 0 & \cdots & 0 \end{bmatrix}, \quad H = \begin{bmatrix} 0 & 1 & 0 & 0 & \dots & 0 \\ 0 & 0 & 0 & 1 & \dots & 0 \\ \vdots & \vdots & \vdots & \vdots & \vdots & \vdots \\ 0 & 0 & 0 & 0 & \dots & 1 \end{bmatrix} \tag{8}$$

In the following, the goal is to propose a systematic approach to estimate the power vector of the CPLs (i.e. $P = \begin{bmatrix} P_1, P_2, \dots, P_Q \end{bmatrix}^T$) and the inductor currents in the face of noisy measurements.

III. EXTENDED KALMAN FILTER

The purpose of this section is to present the development of the EKF, which is used to estimate the value of the CPLs power [27]. To achieve this goal, the unknown CPL power vector, P, should be included in the states of the EKF. To do this, the augmented state vector, including P, is defined as:

$$\dot{x} = \begin{bmatrix} \dot{X} \\ \dot{P}_j \end{bmatrix} \tag{9}$$

Since the dynamic of P is unknown, it is considered as $\dot{P}_j = 0$ for $j = 1, \dots, Q$. Then, the augmented state-space model for the DC MG is as

$$\dot{x} = \begin{bmatrix} \overline{A} X + DP + B_{es} i_{es} + B_s V_{dc} \\ \mathbf{0} \end{bmatrix} = f(x, i_{es}) \tag{10}$$

Considering (9) and the fact that the system measurements, i.e. y, comprise the voltages of the capacitors, y is described as:

$$y = [G \quad 0] \begin{bmatrix} X \\ P_j \end{bmatrix} \tag{11}$$

where $G = \begin{bmatrix} g_{ij} \end{bmatrix}$ and

$$g_{ij} = \begin{cases} 1 & for \quad i = 1, .., Q+1 \; and \; j = 2 \times i \\ 0 & Otherwise \end{cases} \tag{12}$$

Putting (10) and (11) together and considering the system and measurement noises, w and v, respectively, one has

$$\begin{cases} \dot{x} = f(x, i_{es}) + w \\ y = Hx + v \end{cases} \tag{13}$$

where w and v are assumed independent and normally distributed with zero mean and known covariance matrices Q and R, respectively. The obtained state-space model can be discretized using the forward Euler method as:

$$\begin{cases} x_{k+1} = x_k + T_s f(x_k, i_{esk}) + w_k \\ y_k = H x_k + v_k \end{cases} \tag{14}$$

where T_s is the discretizing time and k is the discrete sample number. Since $f(x_k, i_{esk})$ is nonlinear, it cannot be used directly in the EKF algorithm. Rather, its Jacobian, i.e. $F_k = \frac{\partial f}{\partial x}\Big|_{(\hat{x}_k, i_{esk})}$, is used. Then, for a pre-chosen $\hat{x}_0$ and p_0, the EKF algorithm is recursively formulated as follows:

1. **Time Update**

$$\begin{aligned} \hat{x}_k^- &= \hat{x}_{k-1} + T_s f\left(\hat{x}_{k-1}, i_{es(k-1)}\right) \\ p_k^- &= F_{k-1} p_{k-1} F_{k-1}^T + Q_{k-1} \end{aligned} \tag{15}$$

2. **Measurement Update**

$$\begin{aligned} K_k &= p_k^- H_k^T (H_k p_k^- H_k^T + R_k)^{-1} \\ \hat{x}_k &= \hat{x}_k^- + K_k (y_k - H \hat{x}_k^-) \\ p_k &= (I - K_k H_k) p_k^- \end{aligned} \tag{16}$$

where $\hat{x}_k^-$ and $p_k^- \in \mathbb{R}^{(2Q+3)\times 1}$ are the predicted states vector and the predicted covariance matrix of the states, respectively, at the time step k, before considering the measurement. $\hat{x}_k$ and p_k are the estimated states vector and the estimated covariance matrix of the states, respectively, at the time step k, after considering the measurement. $K_k \in \mathbb{R}^{(2Q+3)\times(2Q+2)}$ is the filter gain, which determines how much the predictions should be corrected on the time step k. Finally, the linearized dynamic in (15) is computed as

$$F_k = I + T_s \frac{\partial f(x_k, i_{esk})}{\partial x} \tag{17}$$

This article has been accepted for publication in a future issue of this journal, but has not been fully edited. Content may change prior to final publication. Citation information: DOI 10.1109/JESTPE.2018.2889971, IEEE Journal of Emerging and Selected Topics in Power Electronics

where $\frac{\partial f(x_k,i_{esk})}{\partial x}=\left[\frac{\partial f}{\partial x_j}\quad\frac{\partial f}{\partial x_s}\quad\frac{\partial f}{\partial P_j}\right]$. Using v_{Cj} and v_{Cs} as measurements, the EKF is thus able to estimate P_j, i_{Lj}, i_{Ls} as part of the estimated state vector $\hat{x}_k$.

IV. Nonlinear TS-based MPC Controller

In this section, the design of a nonlinear MPC controller based on a TS fuzzy model of the system is provided.

A. *TS Fuzzy Dynamical Model*

The chosen approach is that of sector nonlinearities, which are known to be able to approximate any smooth nonlinear functions globally or semi-globally [28]. In order to apply the sector nonlinearity approach to the nonlinear part of the dynamical model of the system in (7), i.e. ρ, the model is represented as [29]

$$\begin{cases}\dot{\tilde{X}}=\overline{A}\tilde{X}+D\rho'+B_{es}i_{es}+B_sV_{dc}\\ \tilde{Y}=H\tilde{X}\end{cases} \tag{18}$$

where $\tilde{X}=\left[\tilde{x}_1^T\ \ \tilde{x}_2^T\ \ \dots\ \ \tilde{x}_Q^T\ \ x_s^T\right]^T$, $\rho'=\left[\rho_1',\dots,\rho_Q'\right]^T$ and

$$\overline{A}=\begin{bmatrix}A_1 & 0 & \dots & 0 & A_{1s}\\ 0 & A_2 & \cdots & 0 & A_{2s}\\ \vdots & \vdots & \ddots & \vdots & \vdots\\ 0 & 0 & \cdots & A_Q & A_{Qs}\\ A_{cn} & A_{cn} & \cdots & A_{cn} & A_s\end{bmatrix}, B_{es}=\begin{bmatrix}0\\ \vdots\\ 0\\ b_{es}\end{bmatrix},$$
$$B_s=\begin{bmatrix}0\\ \vdots\\ 0\\ b_s\end{bmatrix}, D=\begin{bmatrix}d_1 & 0 & \dots & 0\\ 0 & d_2 & \cdots & 0\\ \vdots & \vdots & \ddots & \vdots\\ 0 & 0 & \cdots & d_Q\\ 0 & 0 & \cdots & 0\end{bmatrix}, \tag{19}$$
$$H=\begin{bmatrix}0 & 1 & 0 & 0 & \dots & 0\\ 0 & 0 & 0 & 1 & \dots & 0\\ \vdots & \vdots & \vdots & \vdots & \vdots & \vdots\\ 0 & 0 & 0 & 0 & \dots & 1\end{bmatrix},$$
$$\tilde{x}_j=\begin{bmatrix}\tilde{\imath}_{Lj}\\ \tilde{v}_{Cj}\end{bmatrix}, \rho_j'=\frac{\tilde{v}_{Cj}}{v_{Cj0}\left(\tilde{v}_{C,j}+v_{Cj0}\right)}$$

where $\tilde{v}_{Cj}=v_{Cj}-v_{Cj0}, \tilde{\imath}_{Lj}=i_{Lj}-i_{Lj0}$, and v_{Cj0} and i_{Lj0} are the equilibrium points of the DC MG. Based on [14], the j^{th} CPL is locally stable in the region $R_{j,\tilde{x}}=\{\tilde{x}|-w_{2j}\le\tilde{v}_{Cj}\le w_{2j}\}$, where w_{2j} is a positive scalar that can be obtained using LMI techniques [14]. Then, the upper and lower bounds of the j^{th} nonlinear term, i.e. $\frac{\rho_j'}{\tilde{v}_{Cj}}$, are given as $U_{jmin}\le\frac{\rho_j'}{\tilde{v}_{Cj}}\le U_{jmax}$, where $U_{jmin}=\frac{1}{v_{Cj0}(w_{2j}+v_{Cj0})}, U_{jmax}=\frac{1}{v_{Cj0}(v_{Cj0}-w_{2j})}$. Based on the sector nonlinearity approach, the membership functions M_{1j} and M_{2j} are defined such that the following equations are satisfied:

$$\begin{cases}\rho_j'=M_{1j}U_{jmin}\tilde{v}_{Cj}+M_{2j}U_{jmax}\tilde{v}_{Cj}\\ M_{1j}+M_{2j}=1\end{cases} \tag{20}$$

Solving (20) results in

$$M_{1j}=\frac{U_{jmax}\tilde{v}_{Cj}-\rho_j'}{(U_{jmax}-U_{jmin})\tilde{v}_{Cj}}, M_{2j}=1-M_{1j} \tag{21}$$

Then, $r=2^Q$ fuzzy IF-THEN rules will be defined as follows:

Rule 1: IF $\frac{\rho_1'}{\tilde{v}_{C1}}$ is U_{1min}, ⋯, $\frac{\rho_j'}{\tilde{v}_{Cj}}$ is U_{jmin}, ⋯, and $\frac{\rho_Q'}{\tilde{v}_{CQ}}$ is U_{Qmin}
THEN: $\dot{\tilde{X}}=A_1\tilde{X}+B_{es}i_{es}+B_sV_{dc}$

Rule 2: IF $\frac{\rho_1'}{\tilde{v}_{C1}}$ is U_{1min}, ⋯, $\frac{\rho_j'}{\tilde{v}_{Cj}}$ is U_{jmin}, ⋯, and $\frac{\rho_Q'}{\tilde{v}_{CQ}}$ is U_{Qmax}
THEN: $\dot{\tilde{X}}=A_2\tilde{X}+B_{es}i_{es}+B_sV_{dc}$
⋮

Rule r: IF $\frac{\rho_1'}{\tilde{v}_{C1}}$ is U_{1max}, ⋯, $\frac{\rho_j'}{\tilde{v}_{Cj}}$ is U_{jmax}, ⋯, and $\frac{\rho_Q'}{\tilde{v}_{CQ}}$ is U_{Qmax}
THEN: $\dot{\tilde{X}}=A_r\tilde{X}+B_{es}i_{es}+B_sV_{dc}$ (22)

where,

$$\begin{aligned}A_1&=\overline{A}+diag\{D[U_{1min}\ \ \cdots\ \ U_{jmin}\ \ \cdots\ \ U_{Qmin}]^T\}\\ A_2&=\overline{A}+diag\{D[U_{1min}\ \ \cdots\ \ U_{jmin}\ \ \cdots\ \ U_{Qmax}]^T\}\\ &\vdots\\ A_r&=\overline{A}+diag\{D[U_{1max}\ \ \cdots\ \ U_{jmax}\ \ \cdots\ \ U_{Qmax}]^T\}\end{aligned} \tag{23}$$

Also, based on the sector nonlinearity approach, the membership functions associated with each fuzzy rule are defined as [30]

$$\beta_1=\prod_{j=1}^{Q}M_{1j}, \beta_2=\left(\prod_{j=1}^{Q-1}M_{1j}\right)M_{2Q}, \cdots,\ \beta_r=\prod_{j=1}^{Q}M_{2j} \tag{24}$$

By utilizing the singleton fuzzifier, product inference engine, and center of average defuzzifier, the overall TS-fuzzy model is expressed as

$$\dot{\tilde{X}}=\sum_{i=1}^{r}\beta_i\{A_i\tilde{X}+B_{es}i_{es}+B_sV_{dc}\} \tag{25}$$

Now, by applying the Euler discretizing method [31], the overall discrete-time TS fuzzy system is obtained as

$$\begin{cases}\tilde{x}_{k+1}=\sum_{i=1}^{r}\beta_iA_i\tilde{x}_k+\sum_{i=1}^{r}\beta_iB_{es}i_{esk}+\sum_{i=1}^{r}\beta_iB_sV_{dc}\\ \qquad\quad=A_h\tilde{x}_k+B_hu_k+E_h\\ y_k=H\tilde{x}_k\end{cases} \tag{26}$$

where $u_k=i_{esk}$.

B. *TS-Based MPC Controller*

The considered cost function for the MPC is as [32]

$$J(N_p,N_u)=\sum_{j=1}^{N_p}\left[\hat{y}_{k+j|k}-w_{k+j}\right]^2+\sum_{j=1}^{N_u}u_{k+j-1}^2 \tag{27}$$

where N_p and N_u are the prediction and control horizons, respectively, $\hat{y}_{k+j|k}$ is the optimal j-step ahead prediction of the output, and w_{k+j} is a function of a future reference. For the simplicity, in this paper, it is assumed that $w_{k+j}=y_{k+j}$. To obtain the sequence of the control input u_{k+j-1}, it is needed to minimize the cost function J given in (27) with respect to U. This can be done by substituting the obtained TS fuzzy model into the cost function. Then, the values of the predicted outputs $\hat{y}_{k+j|k}$ are calculated as a function of past values of the system characteristics and future control signals. The computed predictions are as:

$$Y=\Psi+\Theta U \tag{28}$$

where $Y=\left[\hat{y}_{k+1|k}\ \ \hat{y}_{k+2|k}\ \ \dots\ \ \hat{y}_{k+N_p|k}\right]^T$, $U=[u_k\ \ u_{k+1}\ \ \dots\ \ u_{k+N_u-1}]^T$ and

This article has been accepted for publication in a future issue of this journal, but has not been fully edited. Content may change prior to final publication. Citation information: DOI 10.1109/JESTPE.2018.2889971, IEEE Journal of Emerging and Selected Topics in Power Electronics

$$\Psi = \begin{bmatrix} HA_h \\ HA_h^2 \\ \vdots \\ HA_h^{N_p} \end{bmatrix} \tilde{x}_k + \begin{bmatrix} HE_h \\ H(I+A_h)E_h \\ \vdots \\ \sum_{i=0}^{N_p-1} HA_h^i E_h \end{bmatrix}, \quad \Theta = \begin{bmatrix} HB_h & \dots & 0 \\ HA_hB_h & \dots & 0 \\ \vdots & \ddots & \vdots \\ HA_h^{N_p-1}B_h & \dots & HA_h^{N_p-N_u}B_h \end{bmatrix} \tag{29}$$

Similarly, the cost function (27) is represented as

$$J(N_p, N_u) = (Y-W)^T(Y-W) + U^TU \tag{30}$$

where $W = \begin{bmatrix} w_{k+1} & w_{k+2} & \dots & w_{k+N_p} \end{bmatrix}^T$. Substituting (28) into (30) yields $J(N_p, N_u) = U^THU + KU + U^TK^T + G$ where, $H = \Theta^T\Theta + I \geq 0$, $K = (\Psi - W)^T\Theta$, $G = (\Psi - W)^T(\Psi - W)$. To minimize J with respect to U, the analytical solution of U can be obtained as

$$U = (\Theta^T\Theta + I)^{-1}\Theta^T(\Psi - W) \tag{31}$$

Remark 1 (overall closed-loop block diagram): The block diagram of the suggested approach is shown in Fig. 3. As can be seen in Fig. 3, the EKF algorithm is utilized to estimate the currents and power of the loads in the DC MG online. Then, these estimations and the measured voltages are deployed in the TS-based MPC controller to compute the optimal value of the injecting current. The EKF algorithm block and the TS-based MPC controller block are explained in sections III and IV, respectively.

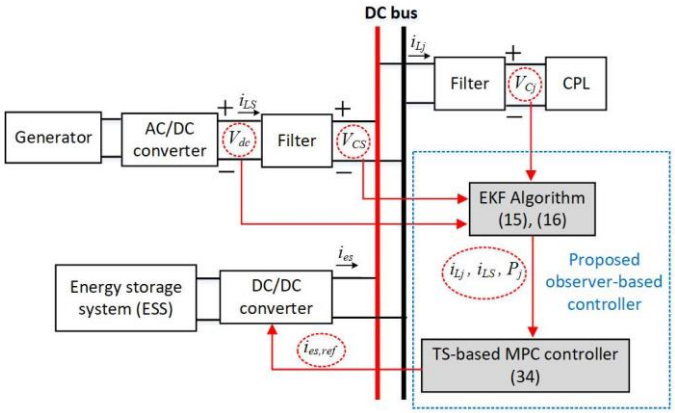

Fig. 3. A simple block diagram of the proposed controller.

Remark 2 (choosing a desired reference in the MPC): As mentioned in [15], by varying the power of the CPL, the equilibrium point of the DC MG changes. However, in order to perform the MPC law in (31), the future reference signal vector, W, must be selected properly. To this aim, a constant value for the CPL's voltage is chosen; then based on its power value, a reference current is chosen for the CPL. Moreover, since the injecting current is utilized to stabilize the DC MG, it is desired to inject no current after DC MG stabilization; In this case, the reference current of the DC source equals to the summation of the CPLs currents. In addition, the reference voltage of the source filter is chosen to be equal to the DC source's voltage. Based on these considerations, the reference vector W is determined.

V. Experimental Results

In this section, experimental results for the proposed adaptive controller are provided. The proposed algorithm has been verified on an experimental set-up equivalent to the Simulink model as shown in Fig. 4. The set-up includes Semikron Power Electronics Teaching Unit, MicroLabBox DS1202 PowerPC DualCore 2 GHz processor board and DS1302 I/O board from dSPACE. The MG parameters used in the experiments are listed in Table I.

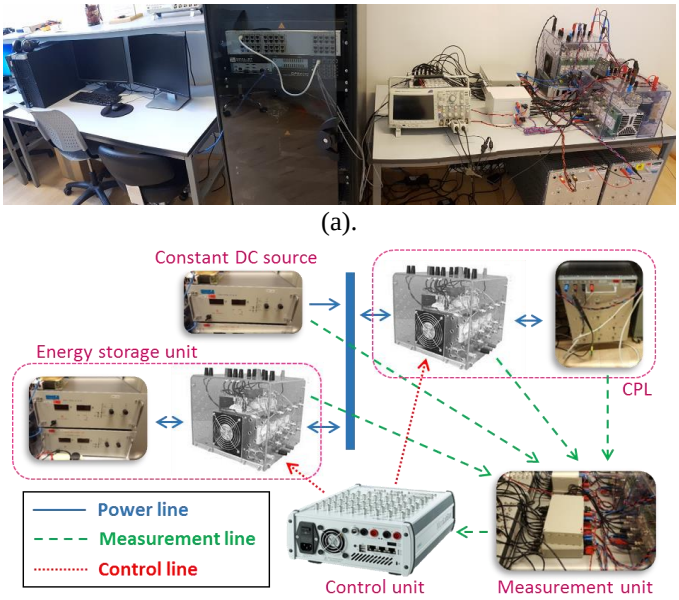

Fig. 4. **(a).** The experimental setup. **(b).** The simplified implantation configuration.

The initial value of the augmented states, i.e. x_0, is guessed based on the available information of the experimental setup as $x_0 = [1\ \ 210\ \ 1\ \ 200\ \ 250]^T$. The covariance matrix of the measurement noise, i.e. R, is obtained based on the iterative testing of sensors. The process noise covariance matrix, i.e. Q, on one hand, corresponds to system noise covariance and on the other hand corresponds to the expected uncertainty in the state-space equations. This could include modelling errors or other uncertainties in the equations themselves. The larger (smaller) value of the Q corresponds to faster (slower) convergence by the expense of larger (smaller) steady-state error [20]. Therefore, the values of R and Q are as

$$R = diag[10^{-2}\ \ 10^{-2}]$$
$$Q = diag[10^{-3}\ \ 10^{-3}\ \ 10^{-3}\ \ 10^{-3}\ \ 10^{-3}] \tag{32}$$

Usually, the initial value of p is diagonal whose diagonal elements are related to the expected variance of the corresponding state. A good guess of the initial values of the states needs a small initial value of the covariance of the states, i.e. p_0. Therefore, p_0 is chosen as

$$p_0 = diag[10^{-1}\ \ 10^{-1}\ \ 10^{-1}\ \ 10^{-1}\ \ 10^{-1}] \tag{33}$$

This article has been accepted for publication in a future issue of this journal, but has not been fully edited. Content may change prior to final publication. Citation information: DOI 10.1109/JESTPE.2018.2889971, IEEE Journal of Emerging and Selected Topics in Power Electronics

To show the effectiveness of the proposed adaptive controller, two scenarios are provided. In the first scenario, the CPL power is chosen so that the open-loop system without a controller is stable. In the second scenario, the CPL power is chosen such that the system without a controller is unstable. In each scenario, the effectiveness of the CPL power estimation and the MPC controller are provided.

Scenario 1: In this scenario P is chosen such that the DC MG is stable without controller and three different cases are considered. In the first case, the DC MG states are shown when no controller is used. In the second case, the DC MG states are investigated when only the MPC controller is used without CPL power estimation. Finally, in the third case, the proposed adaptive controller is deployed.

Case 1: In this case, the controller input, i.e. i_{es}, is considered to be zero. The augmented system states are shown in Fig. 5. As it can be seen, when the CPL power promptly changes, the voltages and currents of the DC MG experience high oscillations in the transient phase. In addition, the voltage of the DC bus drops.

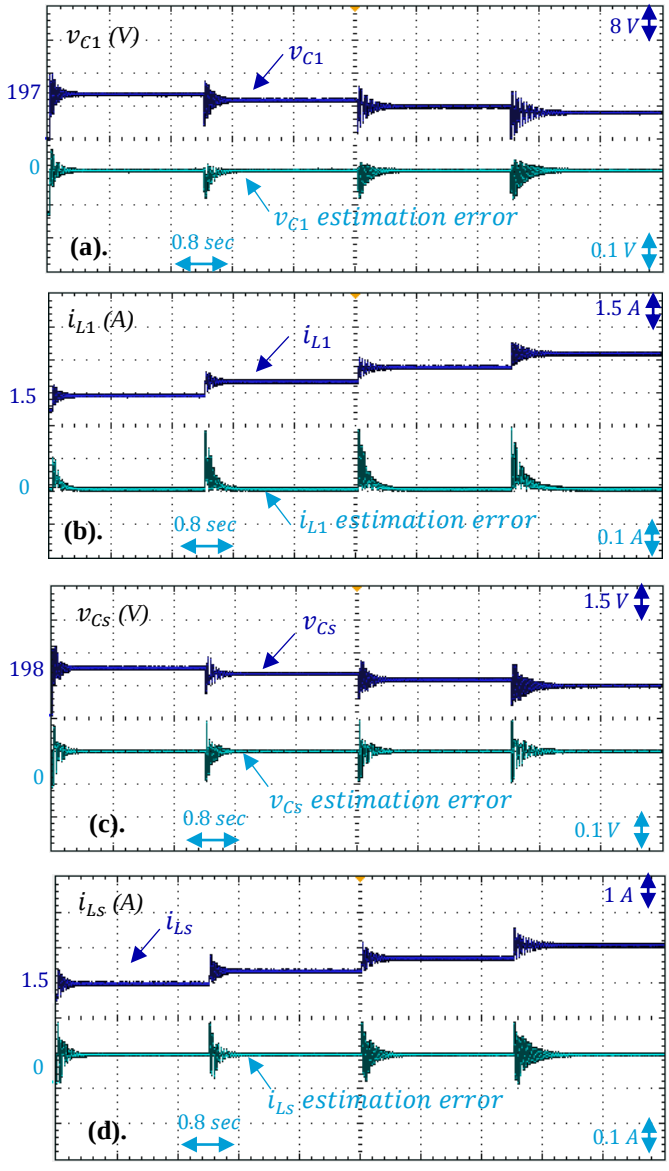

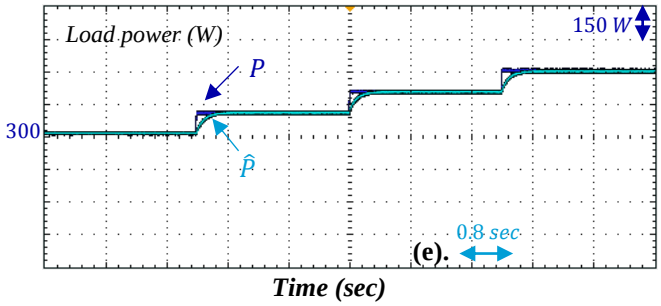

Fig. 5. Augmented system states of Case 1.

Table I: Parameters for the DC MG with one CPL and parameters for the proposed controller

$r_1 = r_s = 1.1\ \Omega$	$v_{C10} = 196.64$	$w_{21} = 130.4$
$C_1 = C_s = 500\ \mu F$	$N_P = N_u = 3$	$V_{dc} = 200\ V$
$L_1 = L_s = 39.5\ mH$		

Case 2: In this case, the MPC controller is employed to stabilize the DC MG. However, the value of CPL power is not estimated and is given in advance. It is assumed that the CPL power is set as $P_1 = 250\ W$, which is less than its actual value given in Fig. 5(e). The state evolutions and controller effort are provided in Fig. 6.

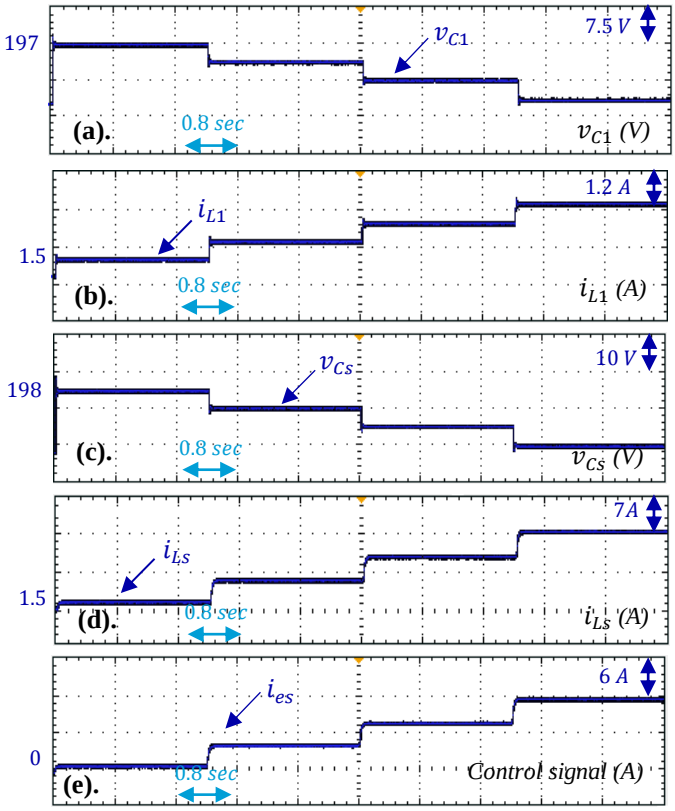

Fig. 6. Augmented system states of Case 2.

From Fig. 6(e) one concludes that a large current is injected to the DC MG. Therefore, the energy storage unit will charge/discharge fast and the battery lifetime is decreased. Furthermore, since the value of the CPL power is not available, a large voltage drop occurs in the DC bus.

This article has been accepted for publication in a future issue of this journal, but has not been fully edited. Content may change prior to final publication. Citation information: DOI 10.1109/JESTPE.2018.2889971, IEEE Journal of Emerging and Selected Topics in Power Electronics

Case 3: In this case, the injecting current is controlled via the adaptive MPC controller that utilizes the CPL power estimation. The augmented system states are shown in Fig. 7. From Fig. 7, one concludes that the adaptive controller stabilizes the DC MG without any oscillations compared to the non-controlled DC MG (Case 1) and keeps the DC bus voltage near the voltage of the DC source compared to the conventional controller (Case 2). Furthermore, the steady state injecting current is much smaller than the Case 2. Thereby, the battery lifetime is improved.

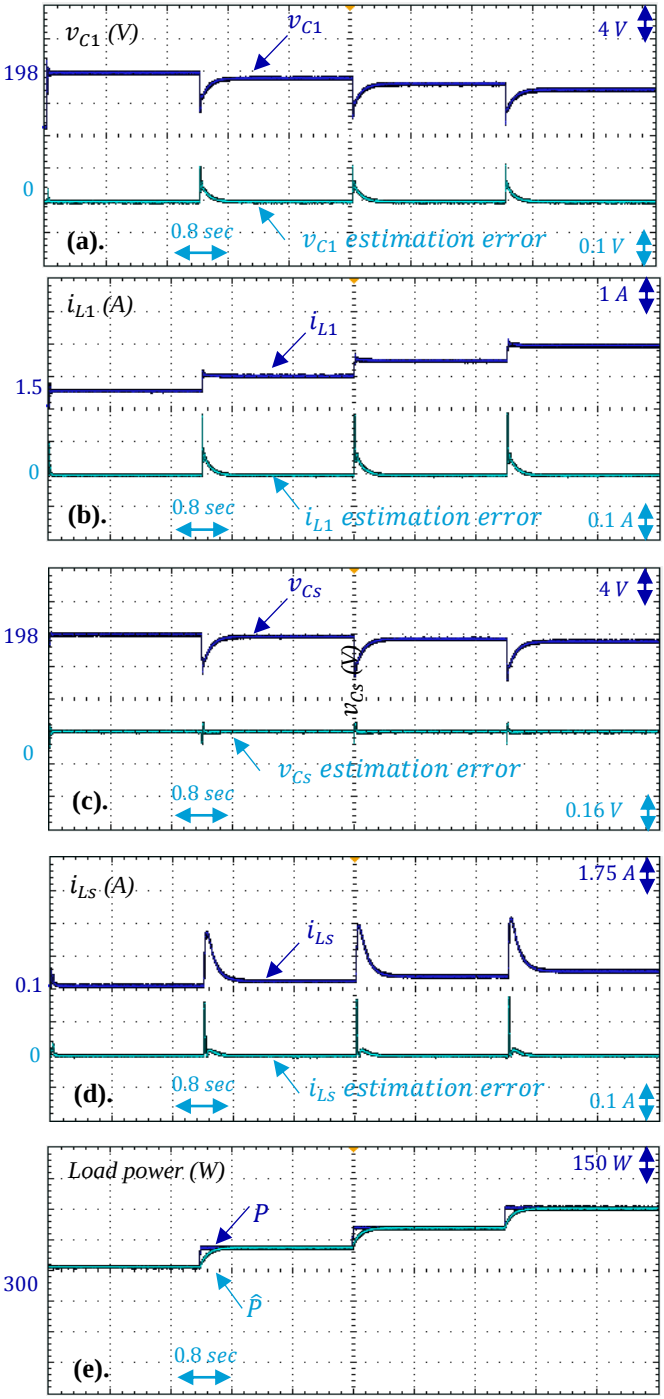

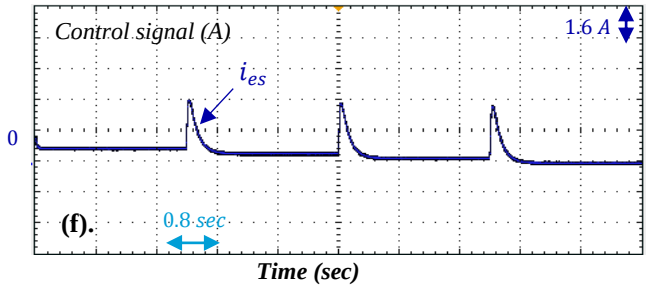

Fig. 7. Augmented system states of Case 3.

Table II provides quantitative comparisons of the three cases of Scenario 1. It reveals the 2-norm of the input and the voltage sag in Case 3 are much smaller than those of Case 2.

Scenario 2: In this case P is chosen as the DC MG is not stable with conventional MPC without CPL estimation cannot stabilize the system. However, by applying the proposed controller the system is stabilized, as can be seen from the closed-loop state evolutions and control effort illustrated in Fig. 8.

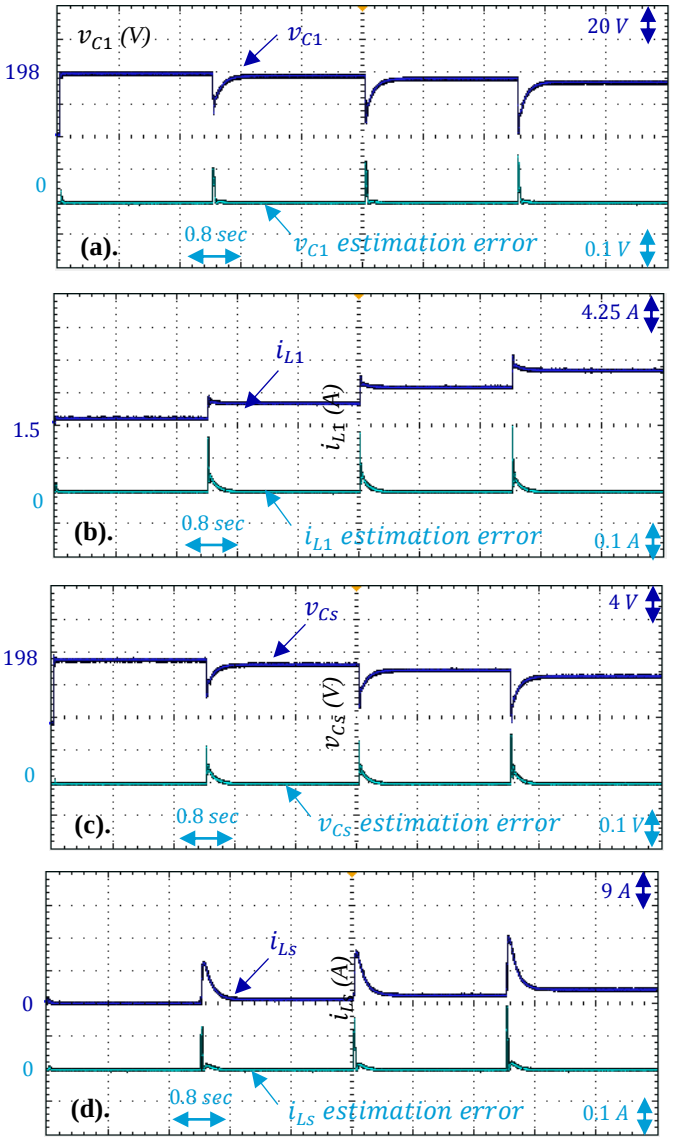

This article has been accepted for publication in a future issue of this journal, but has not been fully edited. Content may change prior to final publication. Citation information: DOI 10.1109/JESTPE.2018.2889971, IEEE Journal of Emerging and Selected Topics in Power Electronics

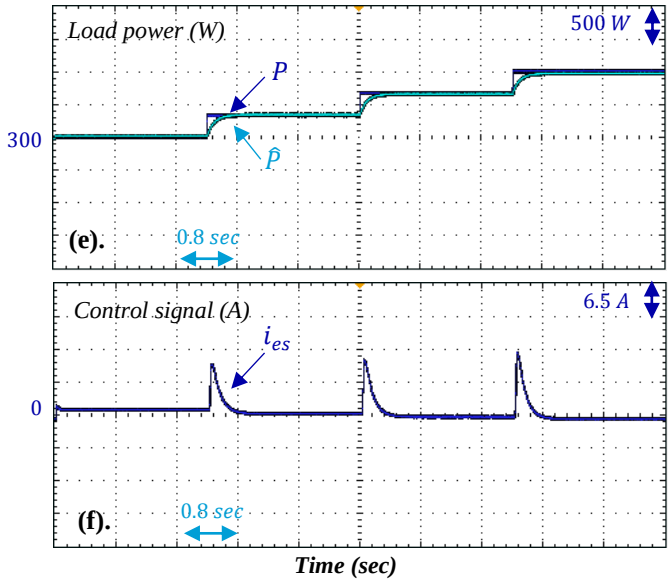

Fig. 8. Augmented system states of Scenario 2.

Table II. Performance and control effort of Scenario 1.

	Case 1	Case 2	Case 3
Overall Voltage drop (Volts)	3.1	15.46	0.91
Transient settling time (2%) (sec)	0.45	0.07	0.43
Norm-2 of the control input	0	2.1290e+3	486.1422

Fig. 8 reveals that the voltages of the DC bus and CPL experience a drop about 20 V when the power of the CPLs suddenly changes about 350 W. These voltage drops happen because it takes about 0.5 sec to estimate the new value of the CPL power.

Remark 3 (General discussion on the advantages of the proposed approach): Generally, nonlinear control methods use a model to design the control law. The performance and effectiveness of these approaches rely on the accuracy and precision of the deployed model. If the modeling is subjected to uncertainties or un-modeled dynamics, the accuracy of the model is degraded, which impairs the performance of the controller. From Case 2, it is inferred that when the value of the CPL power changes from 300 [W] to 600 [W], the conventional MPC is able to stabilize the system but with a poor performance. On the other hand, if the uncertainties or parameter changes of the model are too significant, the closed-loop system may ends up becoming unstable. This is the exact case of time-varying CPLs. Since the value of the power of the CPLs changes over time and their exact values are not estimated by the existing control methods, the accuracy of the model deployed in the MPC reduces and even diminished. In this case, such an approach cannot stabilize the overall system. The reason is that the load power changes too much and the utilized model in the conventional MPC is not accurate enough. However, when the CPL power changes from 300 [W] to 1300 [W], our proposed technique is capable of stabilizing the system.

VI. Conclusion

In this paper, a novel Takagi-Sugeno (TS) fuzzy-based adaptive controller is proposed to regulate the energy storage system (ESS) current complying with the changes of constant power load (CPL) powers included in the DC microgrid (MG) of DC shipboard power systems (SPS). The unknown time-varying CPLs powers are estimated by a developed extended Kalman filter (EKF) algorithm, which is more efficient in cost and performance rather than using sensors. Experimental results show that without estimating the CPL power and the proposed EKF-based MPC, the SPS DC MG may be unstable, experience high oscillations in a transient phase, or be stabilized with a high amplitude injecting current. However, by employing the suggested approach, not only is the transient performance enhanced but the injecting current is also reduced, which results in a better battery lifetime. Furthermore, through the proposed approach, a DC MG with higher values of CPL power can be stabilized compared with the state-of-the-art methods. For the future work, it is suggested to improve the transient performance of the EKF algorithm to estimate the power values of the CPLs faster and provide an enhanced MPC which is more sensitive to the load power variation so that the voltage drops in the DC bus will be decreased. Also, applying more effective nonlinear filters such as cubature Kalman filter (CKF) and unscented Kalman filter (UKF) is recommended.

References

[1] Z. Jin, G. Sulligoi, R. Cuzner, L. Meng, J. C. Vasquez, and J. M. Guerrero, "Next-Generation Shipboard DC Power System: Introduction Smart Grid and dc Microgrid Technologies into Maritime Electrical Netowrks," *IEEE Electrification Mag.*, vol. 4, no. 2, pp. 45–57, Jun. 2016.

[2] M. Khooban, T. Dragicevic, F. Blaabjerg, and M. Delimar, "Shipboard Microgrids: A Novel Approach to Load Frequency Control," *IEEE Trans. Sustain. Energy*, vol. 9, no. 2, pp. 843–852, Apr. 2018.

[3] T. Dragicevic, X. Lu, J. Vasquez, and J. Guerrero, "DC Microgrids-Part I: A Review of Control Strategies and Stabilization Techniques," *IEEE Trans. Power Electron.*, vol. 31, no. 7, pp. 4876–4891, Jul. 2016.

[4] J. Kuseian, "Naval power systems technology development roadmap," *Electr. Ships Off. PMS*, vol. 320, 2013.

[5] D. Bosich, A. Vicenzutti, R. Pelaschiar, R. Menis, and G. Sulligoi, "Toward the future: The MVDC large ship research program," in *AEIT International Annual Conference (AEIT), 2015*, 2015, pp. 1–6.

[6] D. Bosich, M. Gibescu, I. Fazlagic, N. Remijn, and J. de Regt, "Modeling and simulation of an LVDC shipboard power system: Voltage transients comparison with a standard LVAC solution," in *Electrical Systems for Aircraft, Railway, Ship Propulsion and Road Vehicles (ESARS), 2015 International Conference on*, 2015, pp. 1–7.

[7] A. M. Rahimi, G. A. Williamson, and A. Emadi, "Loop-Cancellation Technique: A Novel Nonlinear Feedback to Overcome the Destabilizing Effect of Constant-Power Loads," *IEEE Trans. Veh. Technol.*, vol. 59, no. 2, pp. 650–661, Feb. 2010.

[8] S. Yousefizadeh, J. D. Bendtsen, N. Vafamand, M. H. Khooban, T. Dragicevic, and F. Blaabjerg, "Tracking Control for a DC Microgrid Feeding Uncertain Loads in More Electric Aircraft: Adaptive Backstepping Approach," *IEEE Trans. Ind. Electron.*, 2018.

[9] D. Marx, P. Magne, B. Nahid-Mobarakeh, S. Pierfederici, and

B. Davat, "Large Signal Stability Analysis Tools in DC Power Systems With Constant Power Loads and Variable Power Loads-A Review," *IEEE Trans. Power Electron.*, vol. 27, no. 4, pp. 1773–1787, Apr. 2012.

[10] P. Magne, B. Nahid-Mobarakeh, and S. Pierfederici, "General Active Global Stabilization of Multiloads DC-Power Networks," *IEEE Trans. Power Electron.*, vol. 27, no. 4, pp. 1788–1798, Apr. 2012.

[11] G. Sulligoi, D. Bosich, G. Giadrossi, L. Zhu, M. Cupelli, and A. Monti, "Multiconverter Medium Voltage DC Power Systems on Ships: Constant-Power Loads Instability Solution Using Linearization via State Feedback Control," *IEEE Trans. Smart Grid*, vol. 5, no. 5, pp. 2543–2552, Sep. 2014.

[12] Q. Xu, C. Zhang, C. Wen, and P. Wang, "A Novel Composite Nonlinear Controller for Stabilization of Constant Power Load in DC Microgrid," *IEEE Trans. Smart Grid*, pp. 1–1, 2018.

[13] M. A. Kardan *et al.*, "Improved Stabilization of Nonlinear DC Microgrids: Cubature Kalman Filter Approach," *IEEE Trans. Ind. Appl.*, vol. 54, no. 5, pp. 5104–5112, Sep. 2018.

[14] L. Herrera, W. Zhang, and J. Wang, "Stability Analysis and Controller Design of DC Microgrids With Constant Power Loads," *IEEE Trans. Smart Grid*, vol. 8, no. 2, pp. 881–888, Mar. 2017.

[15] S. Sumsurooah, M. Odavic, and S. Bozhko, "μ Approach to Robust Stability Domains in the Space of Parametric Uncertainties for a Power System With Ideal CPL," *IEEE Trans. Power Electron.*, vol. 33, no. 1, pp. 833–844, Jan. 2018.

[16] J. Liu, W. Zhang, and G. Rizzoni, "Robust Stability Analysis of DC Microgrids With Constant Power Loads," *IEEE Trans. Power Syst.*, vol. 33, no. 1, pp. 851–860, Jan. 2018.

[17] E. Hossain, "Addressing Instability Issues in Microgrids Caused By Constant Power Loads Using Energy Storage Systems," Theses and Dissertations, University of Wisconsin-Milwaukee, Wisconsin, United States, 2016.

[18] K. S. Eom, I. H. Suh, W. K. Chung, and S.-R. Oh, "Disturbance observer based force control of robot manipulator without force sensor," in *Robotics and Automation, 1998. Proceedings. 1998 IEEE International Conference on*, 1998, vol. 4, pp. 3012–3017.

[19] C. Mitsantisuk, K. Ohishi, S. Urushihara, and S. Katsura, "Kalman filter-based disturbance observer and its applications to sensorless force control," *Adv. Robot.*, vol. 25, no. 3–4, pp. 335–353, 2011.

[20] D. Simon, *Optimal state estimation: Kalman, H∞ and nonlinear approaches*. Hoboken, N.J: Wiley-Interscience, 2006.

[21] N. Vafamand, S. Yousefizadeh, M. H. Khooban, J. D. Bendtsen, and T. Dragicevic, "Adaptive TS Fuzzy-Based MPC for DC Microgrids With Dynamic CPLs: Nonlinear Power Observer Approach," *IEEE Syst. J.*, pp. 1–8, 2018.

[22] M. H. Khooban, N. Vafamand, and T. Niknam, "T–S fuzzy model predictive speed control of electrical vehicles," *ISA Trans.*, May 2016.

[23] M. H. Khooban, N. Vafamand, T. Niknam, T. Dragicevic, and F. Blaabjerg, "Model-predictive control based on Takagi-Sugeno fuzzy model for electrical vehicles delayed model," *IET Electr. Power Appl.*, vol. 11, no. 5, pp. 918–934, 2017.

[24] S. Bououden, M. Chadli, S. Filali, and A. El Hajjaji, "Fuzzy model based multivariable predictive control of a variable speed wind turbine: LMI approach," *Renew. Energy*, vol. 37, no. 1, pp. 434–439, Jan. 2012.

[25] N. Jabbour and C. Mademlis, "Online Parameters Estimation and Auto-Tuning of a Discrete-Time Model Predictive Speed Controller for Induction Motor Drives," *IEEE Trans. Power Electron.*, 2018.

[26] L. K. Wong, F. H. F. Leung, and P. K. S. Tam, "Design of fuzzy logic controllers for Takagi–Sugeno fuzzy model based system with guaranteed performance," *Int. J. Approx. Reason.*, vol. 30, no. 1, pp. 41–55, May 2002.

[27] N. Vafamand, S. Yousefizadeh, M. H. Khooban, T. Dragičević, and J. D. Bendtsen, "EKF for Power Estimation of Uncertain Time-varying CPLs in DC Shipboard MGs," presented at the 44th Annual Conference of the IEEE Industrial Electronics Society (IECON 2018), Washington DC, USA, 2018.

[28] H. Ohtake, K. Tanaka, and H. O. Wang, "Fuzzy modeling via sector nonlinearity concept," *Integr. Comput.-Aided Eng.*, vol. 10, no. 4, pp. 333–341, Jan. 2003.

[29] N. Vafamand, M. H. Khooban, T. Dragicevic, and F. Blaabjerg, "Networked Fuzzy Predictive Control of Power Buffers for Dynamic Stabilization of DC Microgrids," *IEEE Trans. Ind. Electron.*, pp. 1–1, 2018.

[30] N. Vafamand, M. H. Asemani, and A. Khayatian, "Robust L1 Observer-based Non-PDC Controller Design for Persistent Bounded Disturbed TS Fuzzy Systems," *IEEE Trans. Fuzzy Syst.*, pp. 1–1, 2017.

[31] B. Stellato, T. Geyer, and P. J. Goulart, "High-Speed Finite Control Set Model Predictive Control for Power Electronics," *IEEE Trans. Power Electron.*, vol. 32, no. 5, pp. 4007–4020, May 2017.

[32] N. Vafamand, M. M. Arefi, M. H. Khooban, T. Dragicevic, and F. Blaabjerg, "Nonlinear Model Predictive Speed Control of Electric Vehicles Represented by Linear Parameter Varying Models with Bias terms," *IEEE J. Emerg. Sel. Top. Power Electron.*, pp. 1–1, 2018.